Three dimensional lattice Boltzmann simulation for mixed convection of nanofluids in the presence of magnetic field

Wenning Zhou[a,*], Yuying Yan[b], Yulei Xie[a], Baiqian Liu[a]

[a]School of Energy and Environmental Engineering, University of Science and Technology Beijing, Beijing 100083, China

[b]Fluids and Thermal Engineering Research Group, Faculty of Engineering, University of Nottingham, University Park, Nottingham NG7 2RD, UK

*Corresponding author:

Dr Zhou, Email: wenningzhou@ustb.edu.cn, Tel: +86 (0) 10 62332730

Abstract

In the present study, a three dimensional thermal lattice Boltzmann model was developed to investigate the flow dynamics and mixed convection heat transfer of Al_2O_3/water nanofluid in a cubic cavity in the presence of magnetic field. The model was first validated with previous numerical and experimental results. Satisfactory agreement was obtained. Then the effects of Rayleigh number, nanoparticle volume fraction, Hartmann number and Richardson number on nanofluid flow dynamics and heat transfer were examined. Numerical results indicate that adding nanoparticles to pure water leads to heat transfer enhancement for low Rayleigh numbers. However, this enhancement might be weakened and even reversed for high Rayleigh numbers. In addition, the results show the external applied magnetic field has an effect of suppressing the convective heat transfer in the cavity. Moreover, the results demonstrate that the Richardson number in mixed convection has significant influences on both streamlines and temperature field.

Keywords: Nanofluid; Magnetic field; Mixed convection; 3D numerical modeling; Lattice Boltzmann method

1. Introduction

Natural/mixed convection heat transfer in a cavity has been the subject of investigation due to its numerous practical applications including heat exchangers, solar collectors, nuclear reactors, energy systems, and many others [1, 2]. Traditional fluids such as water, ethylene glycol and mineral oils usually have low thermal conductivities. To enhance thermodynamic performance, nanofluids, a suspension of nanoparticles into base fluids, possess high thermal conductivity and have been considered as a promising solution [3, 4]. Extensive research has been carried out in this area. Experimental work reported that the thermal conductivity is enhanced by 30% for carbon nanotube nanofluids (2 vol.%) [5]; and heat transfer enhancement up to 40% has been obtained for Al_2O_3/water nanofluid and Al_2O_3/ethylene glycol nanofluid compared to the base fluid [6]. Zhai et al. [7] carried out experiments to study heat transfer enhancement of

Al_2O_3/water nanofluid through a micro heat sink with complex structure. Their results showed that higher volume fraction of nanofluids (0.1-1 vol.%) gives better comprehensive performance of heat transfer.

Recently the effect of external magnetic field on the heat transfer of nanofluids has also received great attention due to their various applications in many fields such as crystal growth, microelectronic devices, medical science, and so forth [8]. Sheikholeslami et al. [9] applied the control volume based finite element method (CVFEM) to simulate magnetohydrodynamics (MHD) natural convection heat transfer between a circular enclosure and an elliptic cylinder. They concluded that the average Nusselt number increases with the increasing of nanoparticle volume fraction and Rayleigh number, but it decreases with the augment of Hartmann number. A meshless point collocation method was developed to investigate MHD natural convection flow in an inclined square enclosure [10]. Their results showed both the strength and orientation of the magnetic field have significant effects on the flow and temperature fields. Selimefendigil et al. [11] recently used the finite element method to study mixed convection entropy generation of CuO/water nanofluid under the influence of inclined magnetic fields. They found that the average Nusselt number decreases with the increasing of Richardson number and Hartmann number. A finite difference scheme was developed to investigate MHD mixed convection over an isothermal circular cylinder in the presence of an aligned magnetic field [12]. They claimed that the fluid flow with large mixed convection can be better controlled with the help of external applied magnetic field.

In the past decade, the lattice Boltzmann method (LBM) has been proposed as a powerful numerical tool for simulating complex multiphase flow [13, 14], electoosmotic flows [15, 16], heat transfer [17, 18], reactive transport [19], and so forth. One can refer to the recent reviews in this area [20-22]. The kinetic nature of LBM gives it many advantages including the simplicity of programming, the parallelism of the algorithm and the capability of incorporating complex microscopic interactions [20]. The LBM has recently been extended to simulate nanofluids flow and heat transfer phenomena [23]. A LES-based lattice Boltzmann was proposed to study the heat and

mass transfer mechanism of double diffusive natural convection of nanofluid from laminar regimes to turbulent regimes [24]. Ahrar et al. [25] applied the lattice Boltzmann method to investigate a nanofluid filled cavity with sinusoidal temperature boundary condition under the influence of an inclined magnetic field. They found that the influence of nanoparticles for this geometry and boundary condition is highly dependent to Rayleigh and Hartmann numbers. A MRT thermal lattice Boltzmann model was developed to simulate MHD flow and heat transfer of Cu/water nanofluid in an inclined cavity with four heat sources [26]. The results showed that the volume fraction of nanoparticles, Hartmann number and inclination angle of cavity have great influences on flow dynamics and heat transfer. Mahmoudi et al. [27] studied natural convection cooling of a nanofluid subjected to a magnetic field in a cavity with two heat sinks vertically attached to the horizontal walls. They found that the heat sinks positions greatly influence the heat transfer rate. Sheikholeslami et al. [28] conducted a numerical investigation on the effect of horizontal magnetic field on free convection heat transfer in a concentric annulus filled with Al_2O_3/water nanofluid. The results showed that the average Nusselt number increases with the increasing of nanoparticle volume fraction and Rayleigh number, but opposite trend is observed when Hartmann number increases. Chen et al. [29] used the lattice Boltzmann method to investigated the natural and mixed convection of Al_2O_3/water nanofluid in a square enclosure. They found that adding nanoparticles on the properties of nanofluids is enlarged in mixed convection situation. Despite a number of studies on nanofluid heat transfer enhancement have been carried out, most of them were conducted in a 2D model for natural convection. There is still a lack of information regarding MHD mixed convection in a cubic cavity. Therefore, in order to accurately investigate natural/mixed convection of nanofluids, a 3D lattice Boltzmann model for MHD mixed convection heat transfer is desirable.

In this work, we extend our previous studies on nanofluids [30, 31] to investigate mixed convection of nanofluids in the presence of magnetic field in a cubic cavity by developing a 3D LBM model. The effects of Rayleigh number, nanoparticle volume fraction, Hartmann number and Richardson number on nanofluid flow and heat transfer

have been examined in this study. The rest of this paper is organized as follows: Section 2 introduces mathematic formulation for nanofluid and lattice Boltzmann method. Grid independence and code validation are presented in Section 3. Numerical results and discussion for MHD natural/mixed convection heat transfer are included in Section 4. The conclusions are drawn in Section 5.

2. Problem description and mathematic formulation

2.1 Problem description

The schematic of the physical model is illustrated in Fig. 1. The length of each side of the cubic cavity is L. The hot wall and cold wall are located at X=0 and X=1, respectively. The other walls of the investigated domain are assumed to be adiabatic. An external magnetic field with uniform strength B_0 is applied. The orientations of the magnetic field with X axis and Z axis are θ_x and θ_z, respectively. The cavity is filled with Al_2O_3/water nanofluid.

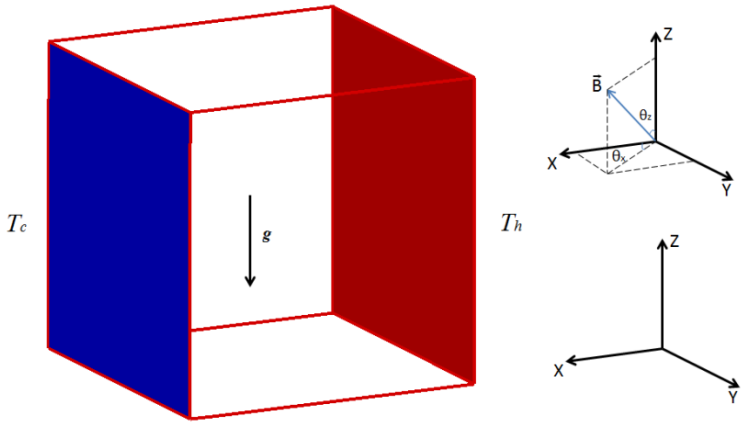

Fig. 1. Schematic domain of the physical model.

2.2 Lattice Boltzmann method

The LBM method with standard three dimensional, nineteen velocities (D3Q19) model for both flow field and temperature is employed in this work. For the sake of completeness, a brief introduction of lattice Boltzmann method is included. One can refer to Refs. [32, 33] for more details. The discretized LBM equations for flow and

temperature field can be written as:

$$f_i(x+c_i\Delta t, t+\Delta t) = f_i(x,t) - \frac{1}{\tau_\nu}(f_i(x,t) - f_i^{eq}(x,t)) + \Delta t F_i \tag{1}$$

$$g_i(x+c_i\Delta t, t+\Delta t) = g_i(x,t) - \frac{1}{\tau_\alpha}(g_i(x,t) - g_i^{eq}(x,t)) \tag{2}$$

where c_i denotes the discrete particle velocity vectors, Δt is the lattice time step which is set to unity. F_i is the external force term in the direction of lattice velocity. τ_ν, τ_α are the relaxation time for the flow and temperature field which are related to kinetic viscosity and thermal diffusivity, i.e., $\nu = (\tau_\nu - 1/2)c_s^2\Delta t$ and $\alpha = (\tau_\alpha - 1/2)c_s^2\Delta t$. f_i^{eq}, g_i^{eq} represent the local equilibrium distribution functions for flow and temperature field which can be calculated by:

$$f_i^{eq} = \rho w_i[1 + \frac{c_i \cdot u}{c_s^2} + \frac{(c_i \cdot u)^2}{2c_s^4} - \frac{u \cdot u}{2c_s^2}] \tag{3}$$

$$g_i^{eq} = w_i T[1 + \frac{c_i \cdot u}{c_s^2}] \tag{4}$$

where c_s is the lattice speed of sound which is equal to $c_s = c/3$, and the discrete velocities for D3Q19, as seen in Fig. 2, are given as follows:

$$c_i = \begin{pmatrix} 0 & 1 & -1 & 0 & 0 & 0 & 0 & 1 & -1 & 1 & -1 & 1 & -1 & 1 & -1 & 0 & 0 & 0 & 0 \\ 0 & 0 & 0 & 1 & -1 & 0 & 0 & 1 & -1 & -1 & 1 & 0 & 0 & 0 & 0 & 1 & -1 & 1 & -1 \\ 0 & 0 & 0 & 0 & 0 & 1 & -1 & 0 & 0 & 0 & 0 & 1 & -1 & -1 & 1 & 1 & -1 & -1 & 1 \end{pmatrix} \tag{5}$$

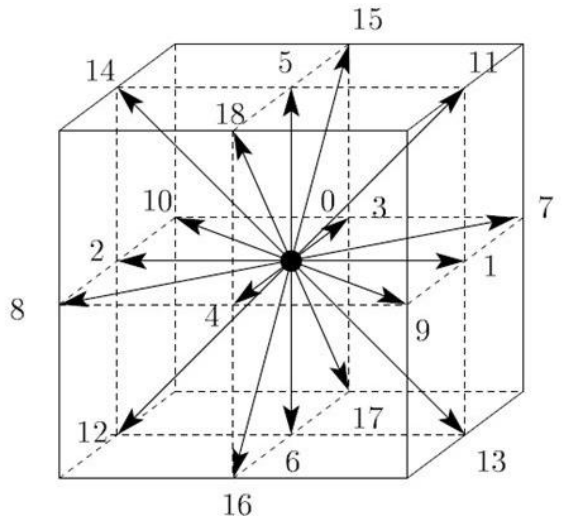

Fig. 2. Discrete velocity for the D3Q19 model.

The weighting factor w_i is defined as:

$$w_i = \begin{cases} 1/3 & i = 0 \\ 1/18 & i = 1:6 \\ 1/36 & i = 7:18 \end{cases} \tag{6}$$

Macroscopic variables such as mass density, momentum density and temperature are defined by sums over the distribution functions, which can be written as:

$$\rho = \sum_i f_i , \quad \rho u = \sum_i f_i c_i , \quad T = \sum g_i \tag{7}$$

2.3 Body forces in lattice Boltzmann model

In this study, it is assumed that the induced magnetic field produced by the motion of an electrically conducting fluid is negligible compared to the applied magnetic field. The external magnetic field only influence the force term. In order to incorporate buoyancy force and magnetic force in the model, the external force term in Eq. (1) in D3Q19 model then can be calculated as [28]:

$$F_i = F_{ix} + F_{iy} + F_{iz} \tag{8}$$

$$\begin{aligned} F_{ix} = {} & 3w_i\rho A[-\cos\theta_z(u\cos\theta_z + w\sin\theta_z\cos\theta_x) \\ & -\sin\theta_z\sin\theta_x(u\sin\theta_z\sin\theta_x - v\sin\theta_z\cos\theta_x)] \end{aligned} \tag{9}$$

$$\begin{aligned} F_{iy} = {} & 3w_i\rho A[\sin\theta_z\cos\theta_x(u\sin\theta_z\sin\theta_x - v\sin\theta_z \\ & \cos\theta_x) - \cos\theta_z(v\cos\theta_z - w\sin\theta_z\sin\theta_x)] \end{aligned} \tag{10}$$

$$\begin{aligned} F_{iz} = {} & 3w_i\rho[g\beta\Delta T + A\sin\theta_z\sin\theta_x(v\cos\theta_z - w\sin\theta_z\sin\theta_x) \\ & + A\sin\theta_z\cos\theta_x(u\cos\theta_z - w\sin\theta_z\cos\theta_x)] \end{aligned} \tag{11}$$

where $A = Ha^2\mu/L^2$, $Ha = LB_0\sqrt{\sigma/\mu}$ is the Hartmann number. θ_x and θ_z are the directions of the external magnetic field. For mixed convection, we assume radiation heat transfer is negligible and the Boussinesq approximation is used. By substituting Eqs. (8-11) to Eq. (1), the effects of buoyancy force and magnetic field on the flow could be taken into consideration.

2.4 Lattice Boltzmann model for nanofluids

In the present work, it is assumed that the base fluid and the nanoparticles are in thermal equilibrium and there is no slip between them. Therefore the nanofluid could be considered to be similar to pure fluid. The thermo-physical properties of the nanofluid

can be obtained:

$$\rho_{nf} = (1-\phi)\rho_f + \phi\rho_p \tag{12}$$

$$(\rho c_p)_{nf} = (1-\phi)(\rho c_p)_f + \phi(\rho c_p)_p \tag{13}$$

$$(\rho\beta)_{nf} = (1-\phi)(\rho\beta)_f + \phi(\rho\beta)_p \tag{14}$$

In the equations above, ρ, c_p, β are the density, heat capacity and thermal expansion coefficient, respectively. ϕ is the volume fraction of nanoparticles and subscripts *nf*, *f* and *p* represent mixture nanofluid, base fluid and nanoparticles, respectively. The dynamic viscosity and effective thermal conductivity of the nanofluid can be determined by the Brinkman model and Maxwell-Garnetts (MG) model [34]:

$$\mu_{nf} = \mu_f / (1-\phi)^{2.5} \tag{15}$$

$$\frac{k_{nf}}{k_f} = \frac{k_p + 2k_f - 2\phi(k_f - k_p)}{k_p + 2k_f + \phi(k_f - k_p)} \tag{16}$$

The local and average Nusselt numbers at the hot and cold walls are determined as:

$$Nu = -\frac{k_{nf}}{k_f}\frac{L}{\Delta T}\frac{\partial T}{\partial x}\bigg|_{x=1} \tag{17}$$

$$Nu_{avg} = \frac{1}{L^2}\int_0^H\int_0^H Nu dy dz \tag{18}$$

where *L* is the height of the square, ΔT is temperature difference between the hot and cold walls. For the convenience, a normalized average Nusselt number is defined as the ratio of Nusselt number at any volume fractions of nanoparticles to that of pure fluid:

$$Nu^*_{avg}(\varphi) = Nu_{avg}(\varphi) / Nu_{avg}(\varphi = 0) \tag{19}$$

Table 1 Thermo-physical properties of different phases of Al_2O_3/water nanofluid

Properties	Base fluid (water)	Nanoparticles (Al_2O_3)
ρ (kg m^{-3})	997.1	3970
c_p (J kg^{-1} K^{-1})	4179	765
μ (kg m^{-1} s^{-1})	0.001004	/
$\beta \times 10^5$ (K^{-1})	21	0.85
k(W m^{-1} K^{-1})	0.613	25

2.5 Governing parameters

The non-dimensional parameters Prandtl number *Pr*, Rayleigh number *Ra* and Mach number *Ma* are defined by:

$$\mathrm{Pr} = \nu / \alpha \tag{20}$$

$$Ra = g\beta\Delta TL^3 \,\mathrm{Pr}/\nu^2 \tag{21}$$

$$Ma = u_c / c_s \tag{22}$$

where $u_c = \sqrt{g\beta\Delta TL}$ is the characteristic velocity. In order to comply with the incompressible limit of the LBM, the Mach number should be less than 0.3. In the present study, Mach number was fixed at *Ma*=0.1.

For mixed convection, a constant velocity u_p was applied at the cold wall in the same direction as the buoyancy force. The Richardson number *Ri* which represents the importance of natural convection relative to the forced convection is defined as:

$$Ri = \frac{Ra}{\mathrm{Pr}\,\mathrm{Re}^2} \tag{23}$$

where $\mathrm{Re} = u_p L / \nu$ is the Reynolds number. Thus, the mixed convection phenomena could be investigated by adjusting different Richardson numbers.

2.6 Boundary conditions

Boundary conditions are extremely important for the accuracy and stability of the simulation results. The unknown distribution functions pointing to the fluid zone at the boundaries nodes should be specified. In the present work, the non-equilibrium extrapolation scheme [35] with second-order accuracy is employed for both the velocity and thermal boundaries. The basic idea of this scheme is to decompose the distribution function at the boundary node into two parts, i.e., equilibrium and non-equilibrium part.

$$f_i(x_w,t) = f_i^{eq}(x_w,t) + f_i^{neq}(x_w,t) \tag{24}$$

The non-equilibrium part is approximately determined by extrapolating from the non-equilibrium distribution at the neighboring fluid node.

$$f_i^{neq}(x_w,t) = f_i(x_f,t) - f_i^{eq}(x_f,t) \tag{25}$$

where x_w is a lattice node on the boundary, and x_f is its nearest neighboring node in the fluid region. $f_i^{eq}(x,t)$ is given by Eq. (3).

The corresponding thermodynamic boundary conditions are implemented in the similar way. The discrete temperature distribution on the boundary is given by:

$$g_i(x_w,t) = g_i^{eq}(x_w,t) + g_i(x_f,t) - g_i^{eq}(x_f,t) \tag{26}$$

3. Grid independence and code validation

Numerical simulations for gird independence were firstly conducted by employing various mesh sizes as shown in Table 2. It is observed that a gird size of 71×71×71 ensures the gird independent solution for natural convection of Al_2O_3/water nanofluid (Ra=1×10^5, $\varphi = 0.04$). The standard of the program convergence in this study is:

$$\max\left|\Phi^{n+1} - \Phi^{n}\right| < 10^{-6} \tag{27}$$

where n is the iteration number and Φ stands for the independent macroscopic variables (U, V, W, T). Therefore, a gird size of 71×71×71 was employed throughout the simulation cases in the present study.

In order to check the reliability and accuracy of the numerical model developed in this study, a validation test of natural convection in an enclosure was carried out. The temperature distributions in the horizontal midline were compared with previous experimental results by Krane and Jessee [36] and numerical work by Khalil Khanafer et al. [37], as shown in Fig. 3. It can be seen that the comparisons show satisfactory agreements.

Table 2 Numerical results at different grids resolution (Ra=1×10^5, $\varphi = 0.04$)

Mesh size	51×51×51	61×61×61	71×71×71	81×81×81
Nu_{avg}	4.219	4.258	4.290	4.293

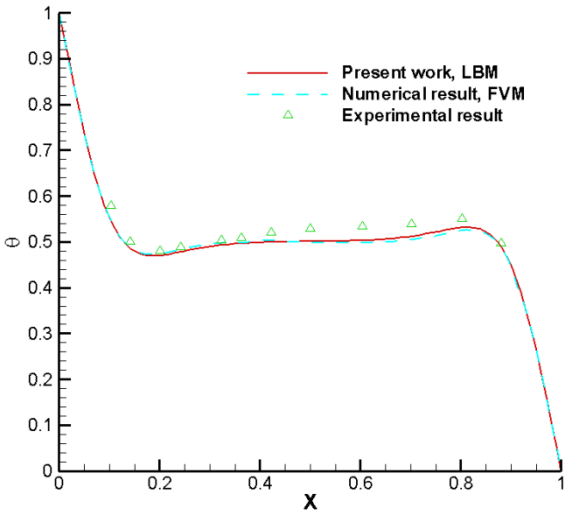

Fig. 3. Comparison of the temperature distribution with other simulation and experimental results (Ra=1.89×10^5, Pr=0.71, $\theta = (T - T_c)/(T_h - T_c)$).

4. Results and discussion

Numerical simulations were carried out to investigate the flow dynamics and heat transfer of Al_2O_3/water nanofluid natural and mixed convection in a cubic cavity in the presence of magnetic field. The computations were conducted for a wide range of Rayleigh numbers (1×10^3-10^6), volume of fractions of nanoparticles (0-6%), Hartmann numbers (0-90) and Richardson numbers (0.01-10). The effects of these parameters on flow dynamics and heat transfer, i.e., streamlines, isotherms, local and average Nusselt numbers were examined.

4.1 Effects of Rayleigh number on fluid flow and heat transfer

Fig. 4 displays the streamlines and isotherms in the cubic cavity for different Rayleigh numbers. Enhancement of heat transfer is found with the increasing of Rayleigh number. As can be seen from the figure, the main vortices stream function increases with the increment of Rayleigh number. This is due to buoyant forces effects become more significant for larger Rayleigh number. The thermal layer becomes much thinner on the side walls as Rayleigh number increases. It means that the heat transfer characteristics in the cubic cavity transform from conduction dominant to convection dominant as Rayleigh number increases.

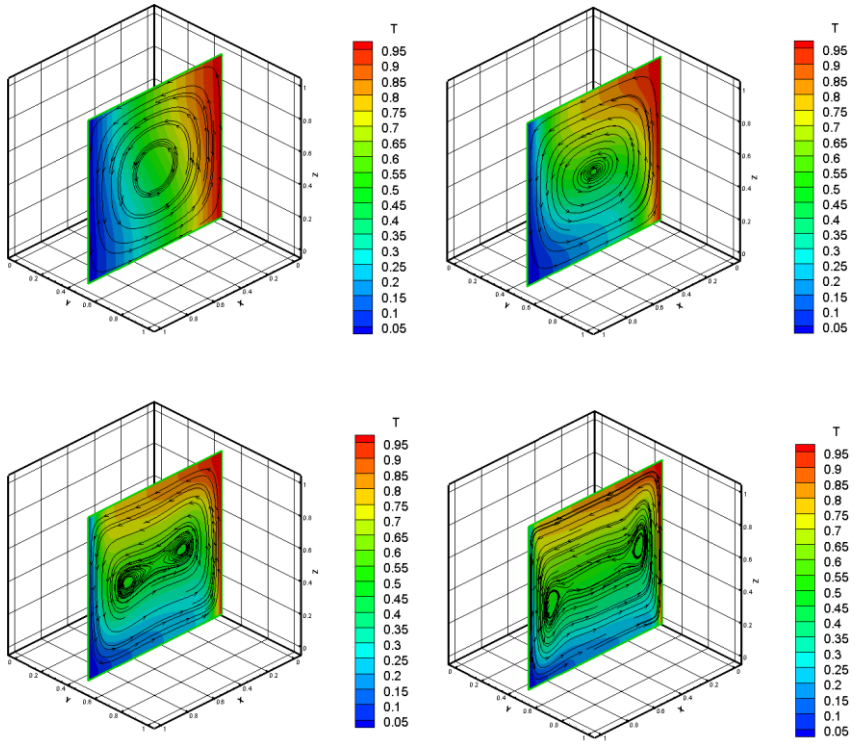

Fig. 4. Streamlines and isotherms for different Rayleigh numbers (a) Ra=1×10^3, (b) Ra=1×10^4, (c) Ra=1×10^5, (d) Ra=1×10^6 ($\varphi = 0.04$).

4.2 Effects of volume fractions of nanoparticles

Fig. 5 presents the effects of volume fractions of nanoparticles on isotherms of nanofluids natural convection in a cubic cavity. Four simulation cases, i.e., $\varphi = 0$, 2%, 4%, 6%, were carried out. It is observed that adding nanoparticles into base fluid enhances energy exchange rates in the fluid and consequently results in the heat transfer enhancement. However, as Rayleigh number increases, the enhancement may be weakened, as shown in Fig. 6. The reason is due to adding nanoparticles to base fluid leads to not only the increase of the thermal conductivity but also the viscosity of the fluid, which results in the reduction of convective heat transfer coefficient and thus decrease of the average Nusselt number. It can be concluded that at lower Rayleigh numbers, i.e., the dominant heat transfer regime is conduction, adding nanoparticles will enhance heat transfer. While with higher Rayleigh numbers where the flow and heat transfer characteristics of nanofluids are more sensitive to viscosity thermal

conductivity, adding nanoparticles has little effect on heat transfer enhancement or may decrease the total heat transfer rate. Similar results were found in the work [38].

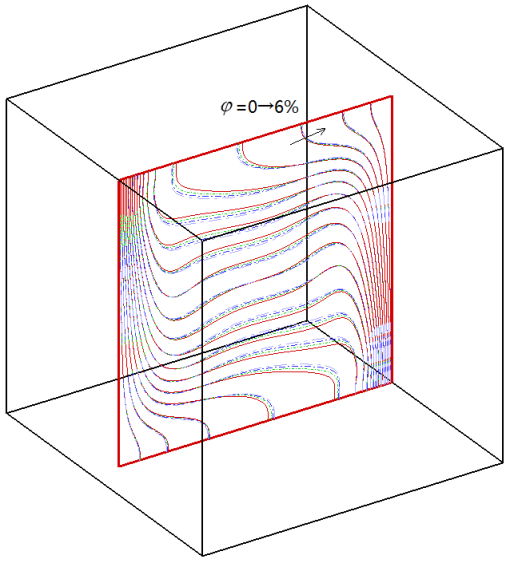

Fig. 5. Isotherms for different volume fractions, $\varphi = 0$, 2%, 4%, 6%, $Ra=1\times10^5$.

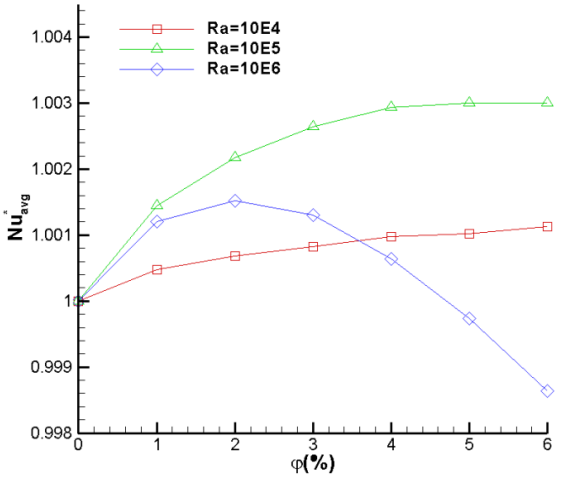

Fig. 6. Variation of the normalized average Nusselt number with nanoparticle volume fraction for $Ra=1\times10^4$-10^6.

4.3 Effects of magnetic field on heat transfer

In order to investigate the effects of external applied magnetic field on heat transfer, a series of simulation tests were carried out. Fig. 7 presents the effects of Hartmann number on isotherms. It is observed the isotherms become parallel to the side wall as

Hartmann number increases. It is due to the increase of Hartmann number leads to increasing Lorentz force, which results in the domination of conduction heat transfer. In other words, the convective heat transfer is suppressed. Fig. 8 illustrates the variation of average Nusselt number with Hartmann number at different Rayleigh numbers. As can be seen in the figure, in contrast to the augmentation of the Rayleigh number the increase of the Hartmann number decreases the heat transfer rate. It is also found that the magnetic field effect is more pronounced for high Rayleigh number.

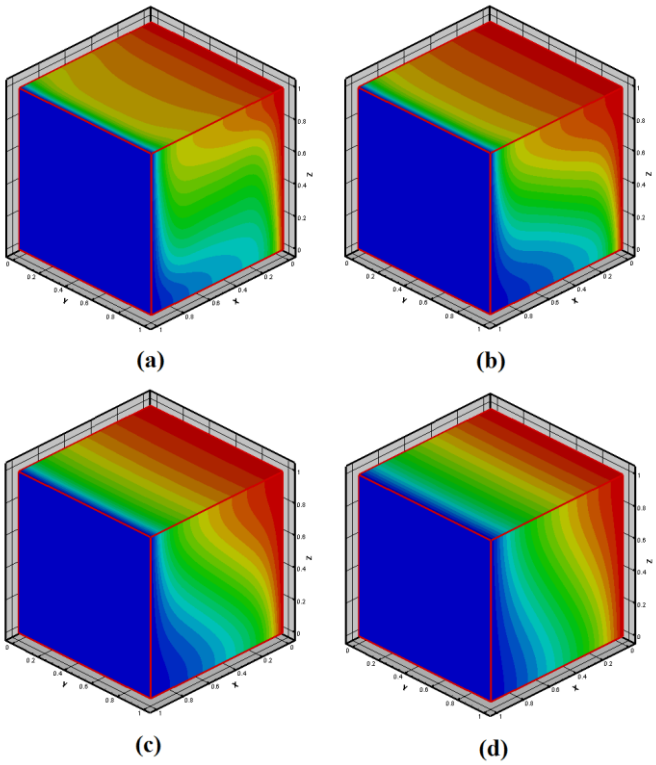

Fig. 7. Effects of Hartmann number (a) *Ha*=0, (b) *Ha*=30, (c) *Ha*=60, (d) *Ha*=90 on isotherms ($Ra=1\times10^5$, $\varphi=4\%$).

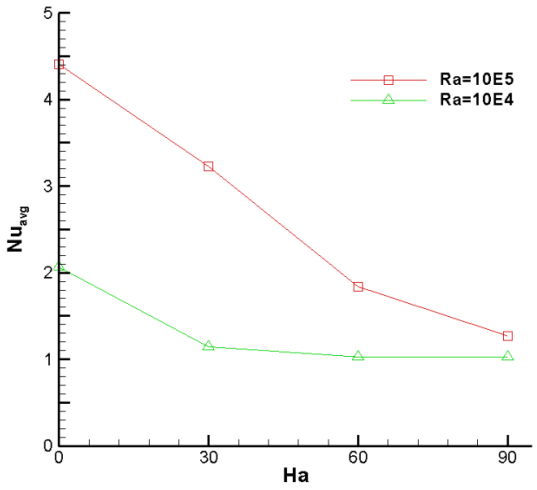

Fig. 8. Variation of average Nusselt number with Hartmann number for different Rayleigh numbers.

Fig. 9 shows the effects of Hartmann number on local Nusselt number of the hot wall. As seen in the figure, the maximum of local Nusselt number significantly decreases with the increase of Hartmann number. It means that the thermal layer thickness increases with the increasing of Hartmann number, indicating the heat transfer is suppressed in this situation. Fig. 10 plots the variation of average Nusselt number with the orientation θ_z of the magnetic field with Z axis when θ_x is fixed at 0°. It is observed that the effect of the orientation of the external magnetic field on the average Nusselt number is nearly symmetrical about the direction θ_z =90°, i.e., horizontal magnetic field. As can be seen in the figure, the average Nusselt number first decreases with the increase orientation θ_z from 0° to 90°, and then increases when the orientation θ_z further increases to 180°. The results indicate that different orientations of external magnetic field exert different degrees of influence on suppressing heat transfer.

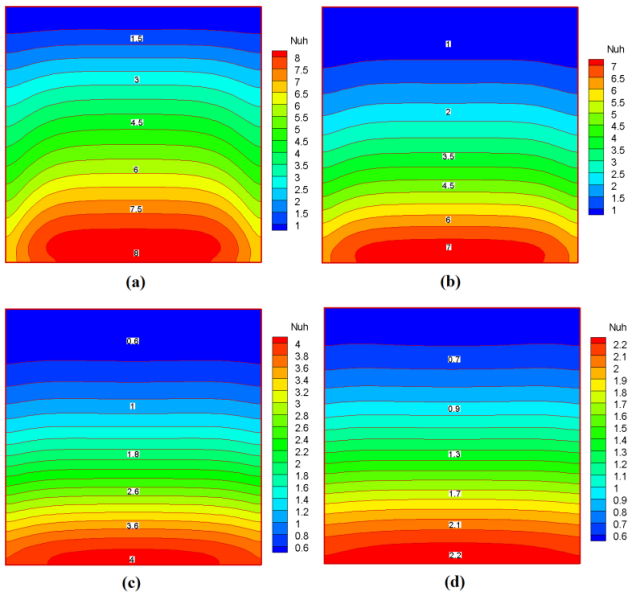

Fig. 9. Effects of Hartmann number (a) *Ha*=0, (b) *Ha*=30, (c) *Ha*=60, (d) *Ha*=90 on local Nusselt number of the hot wall (Ra=1×10^5, φ=4%).

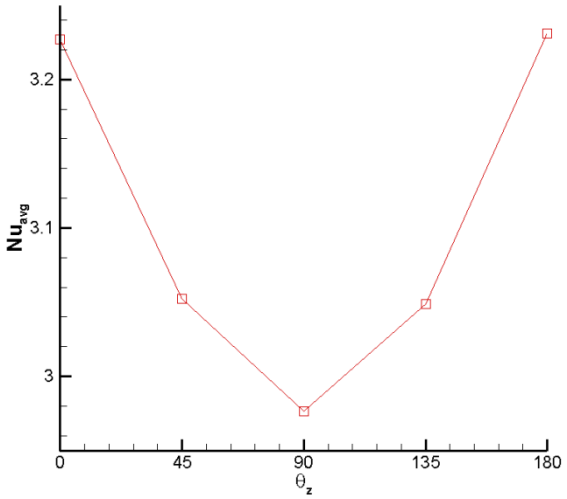

Fig. 10. Variation of average Nusselt number with the orientation of the magnetic field with Z axis (θ_x=0).

4.4 Effects of Richardson number on heat transfer

To study the effects of Richardson number on the heat transfer performances, three Richardson numbers (Ri=0.1, 1, 10) were examined for different Rayleigh numbers (Ra=1×10^4-10^6). Fig. 11 displays the effects of Richardson number on the streamlines

and isotherms of nanofluid at Ra=1×10^5, $\varphi = 0.04$. It is found that the temperature field shows an approximate symmetry when Richardson number is 10, expressing natural convection domination in this case. As Richardson number decreases, forced convection becomes more important and dominates when Ri<1. As seen in Fig. 11, both streamlines and temperature field are greatly affected by Richardson number. Fig. 12 demonstrates the variation of average Nusselt number with Richardson number for different Rayleigh numbers. It is observed that Richardson number has great influences on the average Nusselt number in all simulation cases. A decrease of Richardson number, i.e., a more significant role of forced convection, leads to heat transfer enhancement. In addition, the enhancement is more pronounced for higher Rayleigh number, as shown in Fig. 12. This may provide helpful instructions in heat transfer enhancement in a cubic cavity.

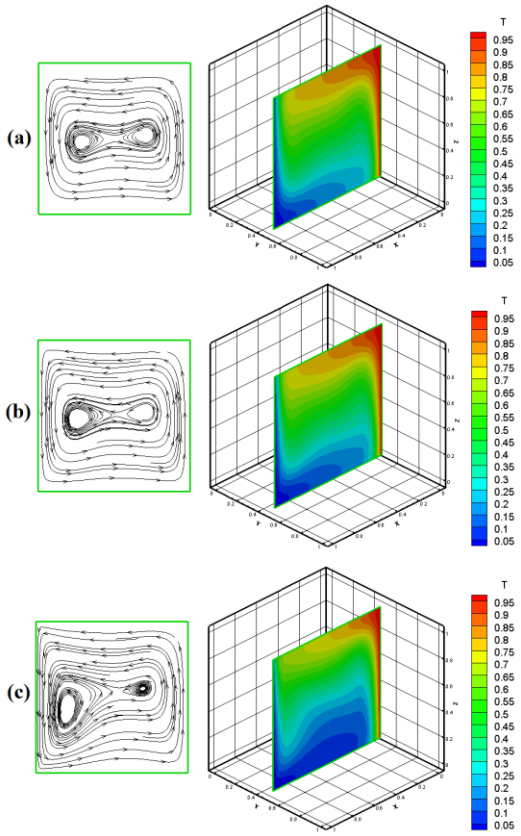

Fig. 11. Streamlines and isotherms for different Richardson numbers (a) Ri=10, (b) Ri=1, (c) Ri=0.1 (Ra=1×10^5, $\varphi = 0.04$).

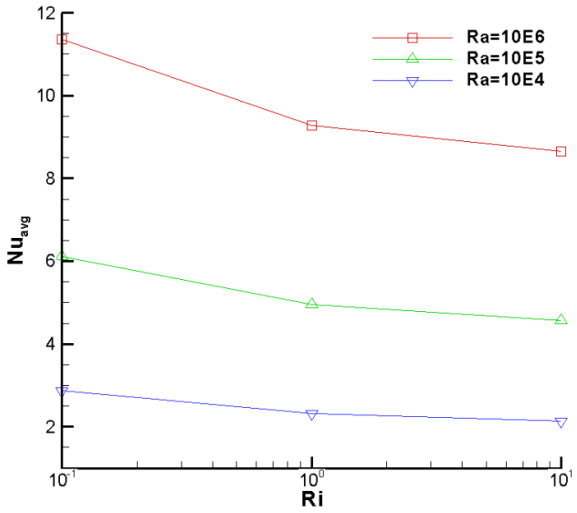

Fig. 12. Variation of average Nusselt number with Richardson number for different Rayleigh numbers.

5. Conclusions

In the present work, natural and mixed convection of Al_2O_3/water nanofluid in a cubic cavity in the presence of magnetic field are numerically investigated using a 3D lattice Boltzmann model. The effects of nanoparticle volume fraction Rayleigh number, Hartmann number, and Richardson number on the flow and heat transfer characteristics have been examined. The following conclusions can be drawn.

(1) Adding nanoparticles of Al_2O_3 into pure water improves natural convection heat transfer in a cubic cavity. However, the effect of convective heat transfer enhancement is more pronounced at low Rayleigh numbers. The enhancement will be weakened and even reversed at high Rayleigh numbers.

(2) In contrast to Rayleigh number, the increase of Hartmann number decreases the heat transfer rate. This effect is more pronounced at high Rayleigh numbers. In addition, the influences of external magnetic field on heat transfer vary with different orientations.

(3) In terms of mixed convection, an improvement of the heat transfer is found as the decrease of Richardson number. Moreover, the results show that Richardson number also has great impacts on both temperature field and streamlines, especially for the case $Ri<1$.

Acknowledgements

This work is financially supported by the Fundamental Research Funds for the Central Universities under Grant No. FRF-TP-15-081A1.

Nomenclature

B Magnetic field

c lattice speed

c_i discrete particle speeds

c_s speed of sound

c_p specific heat capacity

f_i density distribution function

f^{eq} equilibrium distribution function of f_i

F_i forcing term

g gravitational acceleration

g_i energy distribution function

k effective thermal conductivity

L length of cavity

Ma Mach number

Nu Nusselt number

Pr Prandtl number

Ra Rayleigh number

Ha Hartmann number

Ri Richardson number

u_p constant velocity at cold wall

T temperature

w_i weighting factor

Greek Symbols

τ relaxation time

ρ density

ϕ nanoparticle volume fraction

θ magnetic field orientation

μ dynamic viscosity

ν kinetic viscosity

α thermal diffusivity

References

[1] H.F. Oztop, K. Al-Salem, A review on entropy generation in natural and mixed convection heat transfer for energy systems, Renewable and Sustainable Energy Reviews, 16(1) (2012) 911-920.

[2] V.I. Polezhaev, M.N. Myakshina, S.A. Nikitin, Heat transfer due to buoyancy-driven convective interaction in enclosures: Fundamentals and applications, Int J Heat Mass Tran, 55(1–3) (2012) 156-165.

[3] W. Daungthongsuk, S. Wongwises, A critical review of convective heat transfer of nanofluids, Renewable and Sustainable Energy Reviews, 11(5) (2007) 797-817.

[4] L. Godson, B. Raja, D. Mohan Lal, S. Wongwises, Enhancement of heat transfer using nanofluids--An overview, Renewable and Sustainable Energy Reviews, 14(2) (2010) 629-641.

[5] M.S. Liu, M. Ching-Cheng Lin, I. Huang, Enhancement of thermal conductivity with carbon nanotube for nanofluids, Int Commun Heat Mass, 32(9) (2005) 1202-1210.

[6] S.M. Peyghambarzadeh, S.H. Hashemabadi, S.M. Hoseini, M. Seifi Jamnani, Experimental study of heat transfer enhancement using water/ethylene glycol based nanofluids as a new coolant for car radiators, Int Commun Heat Mass, 38(9) (2011) 1283-1290.

[7] Y.L. Zhai, G.D. Xia, X.F. Liu, Y.F. Li, Heat transfer enhancement of Al2O3-H2O nanofluids flowing through a micro heat sink with complex structure, Int Commun Heat Mass, 66 (2015) 158-166.

[8] A.E. Kabeel, E.M.S. El-Said, S.A. Dafea, A review of magnetic field effects on flow and heat transfer in liquids: Present status and future potential for studies and applications, Renewable and Sustainable Energy Reviews, 45 (2015) 830-837.

[9] M. Sheikholeslami, M. Gorji Bandpy, R. Ellahi, M. Hassan, S. Soleimani, Effects of MHD on Cu–water nanofluid flow and heat transfer by means of CVFEM, J Magn

Magn Mater, 349 (2014) 188-200.

[10] G.C. Bourantas, V.C. Loukopoulos, MHD natural-convection flow in an inclined square enclosure filled with a micropolar-nanofluid, Int J Heat Mass Tran, 79 (2014) 930-944.

[11] F. Selimefendigil, H.F. Öztop, A.J. Chamkha, MHD mixed convection and entropy generation of nanofluid filled lid driven cavity under the influence of inclined magnetic fields imposed to its upper and lower diagonal triangular domains, J Magn Magn Mater, 406 (2016) 266-281.

[12] S. Udhayakumar, A.D. Abin Rejeesh, T.V.S. Sekhar, R. Sivakumar, Numerical investigation of magnetohydrodynamic mixed convection over an isothermal circular cylinder in presence of an aligned magnetic field, Int J Heat Mass Tran, 95 (2016) 379-392.

[13] Y.Q. Zu, S. He, Phase-field-based lattice Boltzmann model for incompressible binary fluid systems with density and viscosity contrasts, Phys Rev E, 87(4) (2013) 043301.

[14] Z. Yu, L.S. Fan, Multirelaxation-time interaction-potential-based lattice Boltzmann model for two-phase flow, Phys Rev E, 82(4) (2010) -.

[15] B. Li, W. Zhou, Y. Yan, Z. Han, L. Ren, Numerical Modelling of Electroosmotic Driven Flow in Nanoporous Media by Lattice Boltzmann Method, Journal of Bionic Engineering, 10(1) (2013) 90-99.

[16] Y. Zu, Y. Yan, Numerical simulation of electroosmotic flow near earthworm surface, Journal of Bionic Engineering, 3(4) (2006) 179-186.

[17] W. Li, X. Zhou, B. Dong, T. Sun, A thermal LBM model for studying complex flow and heat transfer problems in body-fitted coordinates, Int J Therm Sci, 98 (2015) 266-276.

[18] Y. Yan, Y. Zu, Numerical simulation of heat transfer and fluid flow past a rotating isothermal cylinder-A LBM approach, Int J Heat Mass Tran, 51(9-10) (2008) 2519-2536.

[19] L. Chen, Q. Kang, Q. Tang, B.A. Robinson, Y.-L. He, W.-Q. Tao, Pore-scale simulation of multicomponent multiphase reactive transport with dissolution and

precipitation, Int J Heat Mass Tran, 85 (2015) 935-949.

[20] Q. Li, K.H. Luo, Q.J. Kang, Y.L. He, Q. Chen, Q. Liu, Lattice Boltzmann methods for multiphase flow and phase-change heat transfer, Progress in Energy and Combustion Science, (2015).

[21] L. Chen, Q. Kang, Y. Mu, Y.-L. He, W.-Q. Tao, A critical review of the pseudopotential multiphase lattice Boltzmann model: Methods and applications, Int J Heat Mass Tran, 76 (2014) 210-236.

[22] Y.Y. Yan, Y.Q. Zu, B. Dong, LBM, a useful tool for mesoscale modelling of single-phase and multiphase flow, Appl Therm Eng, 31(5) (2011) 649-655.

[23] N.A.C. Sidik, R. Mamat, Recent progress on lattice Boltzmann simulation of nanofluids: A review, Int Commun Heat Mass, 66 (2015) 11-22.

[24] S. Chen, B. Yang, K.H. Luo, X. Xiong, C. Zheng, Double diffusion natural convection in a square cavity filled with nanofluid, Int J Heat Mass Tran, 95 (2016) 1070-1083.

[25] A.J. Ahrar, M.H. Djavareshkian, Lattice Boltzmann simulation of a Cu-water nanofluid filled cavity in order to investigate the influence of volume fraction and magnetic field specifications on flow and heat transfer, Journal of Molecular Liquids, 215 (2016) 328-338.

[26] T. Zhang, D. Che, Double MRT thermal lattice Boltzmann simulation for MHD natural convection of nanofluids in an inclined cavity with four square heat sources, Int J Heat Mass Tran, 94 (2016) 87-100.

[27] A. Mahmoudi, I. Mejri, A. Omri, Study of natural convection cooling of a nanofluid subjected to a magnetic field, Physica A: Statistical Mechanics and its Applications, 451 (2016) 333-348.

[28] M. Sheikholeslami, M. Gorji-Bandpy, D.D. Ganji, Numerical investigation of MHD effects on Al2O3–water nanofluid flow and heat transfer in a semi-annulus enclosure using LBM, Energy, 60 (2013) 501-510.

[29] C.-L. Chen, S.-C. Chang, C.o.-K. Chen, C.-K. Chang, Lattice Boltzmann simulation for mixed convection of nanofluids in a square enclosure, Appl Math Model, 39(8) (2015) 2436-2451.

[30] W.N. Zhou, Y.Y. Yan, Numerical Investigation of the Effects of a Magnetic Field on Nanofluid Flow and Heat Transfer by the Lattice Boltzmann Method, Numerical Heat Transfer, Part A: Applications, 68(1) (2015) 1-16.

[31] W.N. Zhou, Y.Y. Yan, J.L. Xu, A lattice Boltzmann simulation of enhanced heat transfer of nanofluids, Int Commun Heat Mass, 55(0) (2014) 113-120.

[32] R. Nourgaliev, T. Dinh, T. Theofanous, D. Joseph, The lattice Boltzmann equation method: theoretical interpretation, numerics and implications, Int J Multiphas Flow, 29(1) (2003) 117-169.

[33] P. Lallemand, L.S. Luo, Theory of the lattice Boltzmann method: Dispersion, dissipation, isotropy, Galilean invariance, and stability, Phys Rev E, 61(6) (2000) 6546-6562.

[34] B. Ghasemi, S.M. Aminossadati, A. Raisi, Magnetic field effect on natural convection in a nanofluid-filled square enclosure, Int J Therm Sci, 50(9) (2011) 1748-1756.

[35] Z. Guo, C. Zheng, B. Shi, An extrapolation method for boundary conditions in lattice Boltzmann method, Phys Fluids, 14 (2002) 2007.

[36] R.J. Krane, J. Jessee, Some detailed field measurements for a natural convection flow in a vertical square enclosure, in: 1st ASME-JSME Thermal Engineering Joint Conference, ASME, New York, 1983, pp. 323-329.

[37] K. Khanafer, K. Vafai, M. Lightstone, Buoyancy-driven heat transfer enhancement in a two-dimensional enclosure utilizing nanofluids, Int J Heat Mass Tran, 46(19) (2003) 3639-3653.

[38] Y. He, C. Qi, Y. Hu, B. Qin, F. Li, Y. Ding, Lattice Boltzmann simulation of alumina-water nanofluid in a square cavity, Nanoscale Research Letters, 6(1) (2011) 184.